BIOCHEMISTRY

 Volume 45, Number 45 November 14, 2006

Articles

Thermodynamic Basis for Redox Regulation of the Yap1 Signal Transduction Pathway†

Jeremy T. Mason,‡ Sung-Kun Kim,‡ David B. Knaff,‡ and Matthew J. Wood*,§

Department of Chemistry and Biochemistry, Center for Biotechnology and Genomics, Texas Tech University, Lubbock, Texas 79409-1061, and Department of Environmental Toxicology, University of California—Davis, Davis, California 95616

Received June 7, 2006; Revised Manuscript Received August 7, 2006

ABSTRACT: The Yap1 oxidative stress signal transduction pathway found in *Saccharomyces cerevisiae* is redox-regulated. We have examined the thermodynamic basis of the disulfide/dithiol couples that are involved in the regulation of this pathway. The oxidized form of the Yap1 redox domain (Yap1-RD) fragment, derived from the Yap1 transcription factor, contains two disulfide bonds, one between Cys303 and Cys598 and one between Cys310 and Cys629. Oxidation−reduction titrations reveal the presence of two separate two-electron redox couples in Yap1-RD, with redox midpoint potentials (E_m) of −155 and −330 mV, respectively, at pH 7.0. We measured E_m values of −275 and −265 mV for the two cytoplasmic *S. cerevisiae* thioredoxins, Trx1 and Trx2, respectively, both at pH 7.0. Last, we measured an E_m value of −255 mV for the Cys36−Cys82 disulfide bond at pH 6.0 in the glutathione peroxidase-like enzyme, oxidant receptor protein (Orp1). We were unable to obtain satisfactory redox titration data for Orp1 at pH 7.0, but if the redox-active disulfide of Orp1 exhibits the −59 mV per pH unit dependence for E_m typical of protein disulfides in this pH region, an E_m value of −315 mV can be estimated for Orp1 at pH 7.0 by extrapolation. Together, these data suggest that, at physiological ratios of Trx_{ox}/Trx_{red}, the reduction of both the $E_m = -315$ mV disulfide of Orp1 and the $E_m = -330$ mV disulfide of Yap1 by either Trx1 or Trx2 would be thermodynamically possible.

Oxidative stress is a result of increased levels of reactive oxygen species (ROS),[1] such as superoxide anion, hydrogen peroxide (H_2O_2), and hydroxyl radicals. ROS indiscriminately damages cellular macromolecules such as proteins, nucleic acids, and lipids when they are left unchecked by cellular defense systems (*1*−*4*). ROS have been implicated in several degenerative diseases and the aging process (*5*−*7*). A defense mechanism that organisms have evolved against oxidative stress involves a class of ROS-sensing proteins (*8*−*10*). These proteins are part of signal transduction pathways that when activated by increased ROS levels result in the

† Work carried out at Texas Tech University was supported by a grant (D-0710 to D.B.K.) from the Robert A. Welch Foundation.

* To whom correspondence should be addressed: Department of Environmental Toxicology, University of California—Davis, One Shields Ave., 4138 Meyer Hall, Davis, California 95616. Telephone: 530-754-2271. Fax: 530-752-3394. E-mail: mjwood@ucdavis.edu.

‡ Texas Tech University.

§ University of California—Davis.

[1] Abbreviations: c-CRD, C-terminal cysteine-rich domain; DTT_{red}, reduced dithiothreitol; DTT_{ox}, oxidized dithiothreitol; GSH, reduced glutathione; GSSG, oxidized glutathione; E_h, ambient potential; E_m, midpoint potential; HSQC, heteronuclear single-quantum coherence; MALDI−TOF, matrix-assisted laser desorption ionization−time of flight; mBBr, momobromobimane; n-CRD, N-terminal cysteine-rich domain; NES, nuclear export signal; NMR, nuclear magnetic resonance; Orp1, oxidant receptor protein; PCR, polymerase chain reaction; ROS, reactive oxygen species; SDS−PAGE, sodium dodecyl sulfate−polyacrylamide gel electrophoresis; TCA, trichloroacetic acid; Trx_{ox}, oxidized thioredoxin Trx_{red}, reduced thioredoxin; Yap1-RD, Yap1 redox domain.

10.1021/bi061136y CCC: $33.50
Published on Web 10/20/2006

expression of genes involved in oxidative stress defense.

The budding yeast *Saccharomyces cerevisiae* has provided a valuable eukaryotic model for understanding the molecular and biochemical mechanisms involved in oxidative-stress-induced signal transduction pathways. The major oxidative stress response pathway in *S. cerevisiae* involves the transcription factor Yap1 (*11*). Other proteins involved in this signal transduction pathway include an oxidant receptor protein (Orp1), the Yap1 accessory protein (Ybp1), and thioredoxin (Trx1 and Trx2) (*12*−*14*). The Yap1 oxidative stress response pathway is regulated by a reversible disulfide/dithiol-relay cascade and controls the expression of ∼70 genes in response to hydrogen peroxide treatment (*15*). In unstressed cells, Yap1 exists in its reduced form and is distributed equally throughout the cytoplasm and nucleus because it contains both nuclear localization and nuclear export signals (NES) (*16*−*18*). In response to oxidative stress, Yap1 rapidly forms two disulfide bonds, resulting in the inhibition of the Yap1 interaction with the nuclear export protein, Crm1 (*18*). This leads to Yap1 nuclear accumulation and consequently increased Yap1 target gene expression. Over the course of approximately 30 min, the Yap1 disulfide bonds are reduced and the Yap1 protein redistributes back into the cytoplasm (*19*).

The Yap1 transcription factor forms reversible and transient disulfide bonds between conserved cysteine residues in response to increased levels of H_2O_2. Individual cysteine to alanine point mutations in four Yap1 cysteine residues, Cys303, Cys310, Cys598, and Cys629, are each defective in their response to H_2O_2 (*19*). Biochemical and structural data demonstrated that disulfide bonds exist between Cys303−Cys598 and Cys310−Cys629 and are located within a protease-resistant domain of Yap1 known as the Yap1 redox domain (Yap1-RD) (*20*). The protein structure of Yap1-RD revealed that these two disulfides connect two distant regions of Yap1 known as the N-terminal cysteine-rich domain (n-CRD) and the C-terminal cysteine-rich domain (c-CRD) (*21*). The disulfide-mediated interactions stabilize the tertiary structure of Yap1-RD, resulting in a masked and inhibited Yap1 NES. Reduction of Yap1-RD disulfide bonds results in a considerable loss of secondary and tertiary structure and unmasks the Yap1 NES. One question that the Yap1-RD structure did not answer is how the disulfide bonds are stable in the reducing environment of the cellular cytoplasm and nucleus.

Both glutathione- and thioredoxin-dependent peroxidase enzymes catalyze the reduction of hydrogen peroxide and alkyl hydroperoxides to water or alcohol, respectively (*8*). These enzymes have been the subjects of increased attention lately because of their putative roles in signal transduction pathways that respond to oxidative stress (*22*). The *S. cerevisiae* genome contains three glutathione peroxidase-like enzymes that share sequence homology with mammalian phospholipid glutathione peroxidases (*23*). Of these, glutathione peroxidase 3 (Orp1) has an additional biological function associated with initiation of H_2O_2 signal transduction (*12*). There is genetic and biochemical evidence that H_2O_2-activated Orp1 catalyzes the formation of the Cys303−Cys598 disulfide bond of Yap1. *ORP1* deleted *S. cerevisiae* strains are hypersensitive to H_2O_2 and do not induce Yap1 disulfide bond formation in response to peroxides (*12*). Orp1 can also catalyze the reduction of peroxides through a mechanism that involves a Cys36−Cys82 intramolecular disulfide bond, suggesting that Orp1 has dual functions *in vivo*. Both functions involve the formation of transient intracellular disulfide bonds, and their redox midpoint potentials are unknown. Interestingly, thioredoxin proteins and not glutathione reduce the Orp1 Cys36−Cys82 disulfide bond.

The thioredoxin family of proteins catalyzes the reduction of disulfide bonds *in vivo*, and their negative redox potentials contribute to the overall reducing environment of the cytoplasm and nucleus (*24*). The *S. cerevisiae* genome contains two cytoplasmic thioredoxin genes, *TRX1* and *TRX2*. *TRX2* was one of the first identified gene targets of the Yap1 transcription factor and is among the most highly induced genes in response to oxidative stress (*25*). There are strong genetic and biochemical data that suggest that *TRX1* and *TRX2* have overlapping roles in the reduction of the Yap1 disulfide bonds that transiently form in response to oxidative stress. A GFP−Yap1 fusion protein is constitutively localized to the nucleus in *S. cerevisiae* strains, where both *TRX1* and *TRX2* have been deleted (*13*). In addition, purified Trx2 from *S. cerevisiae* and TrxA from *Escherichia coli* are both able to reduce Yap1 and Orp1 disulfide bonds *in vitro* (*19*, *20*). Therefore, thioredoxins are responsible for the negative regulation of the Yap1 transcription factor activity and are also participants in the catalytic cycle of Orp1, which is itself a positive regulator of Yap1 activity.

The disulfide bonds involved in the Yap1 oxidative stress signal transduction pathway in *S. cerevisiae* are well-defined. However, it is not clear how the redox midpoint potential of each disulfide bond contributes to the regulation of the signal transduction pathway. Particularly in the case of Yap1, it is not understood how, when once formed, the disulfide bonds are transiently stable for 15−30 min in the overall reducing environment of the cytoplasm and nucleus. In this study, we have systematically investigated the thermodynamic basis of the disulfide bond relay pathways that regulate Yap1 transcriptional activity and Orp1 enzymatic activity in response to increased H_2O_2 levels. We have purified components of the Yap1 signal transduction pathway and measured their redox midpoint potentials. These measurements provide a starting point for the development of a thermodynamic model for the H_2O_2 response pathway in *S. cerevisiae*.

MATERIALS AND METHODS

Protein Expression, Purification, and Characterization. Yap1-RD was expressed and purified as previously described (*21*). Recombinant Trx1 and Trx2 proteins were overexpressed in *E. coli* using the pET vector system (Novagen). The *TRX1* and *TRX2* genes were polymerase chain reaction (PCR)-amplified from *S. cerevisiae* genomic DNA and subcloned into the pET-15b vector using the *Nde*I and *Bam*HI restriction sites, resulting in an open-reading frame with an amino-terminal histidine tag. Recombinant Orp1 protein was overexpressed in *E. coli* using the pRSET vector system (Invitrogen). The *ORP1* gene was PCR-amplified from *S. cerevisiae* genomic DNA and subcloned into the pRSET-B vector using the *Bam*HI and *Nco*I restriction sites.

Trx1, Trx2, and Orp1 proteins were overexpressed in the *E. coli* BL21(DE3) pLysS strain. Cell pellets were resuspended in buffer containing 50 mM Na_2PO_4, 300 mM NaCl,

10% (v/v) glycerol, and 5 mM $MgCl_2$ at pH 8.0 and were lysed by either two passages in a French pressure cell at 18 000 psi or sonication. Cell debris was cleared from the supernatant by centrifugation at 28000*g* for 30 min. The clarified supernatant was loaded onto a Ni^{2+}-chelating column (GE Healthcare or Qiagen) attached to a fast protein liquid chromatography (FPLC) system and washed with 150 mL of buffer containing 50 mM Na_2PO_4, 300 mM NaCl, and 10% (v/v) glycerol. 6×Histidine-tagged (His_6 tag) proteins were eluted from the Ni^{2+} column using the same buffer with the addition of 150 mM imidazole. The Trx1 and Trx2 Ni^{2+} eluates were washed and concentrated in 30 mM *N*-2-hydroxyethylpiperazine-*N*′-2-ethanesulfonic acid (Hepes) and 100 mM NaCl at pH 7.0 using Millipore Amicon Ultra 15 mL centrifuge filtration tubes. Concentrated Trx1 and Trx2 Ni^{2+} eluates were loaded onto a Superdex 75 column for further purification. Orp1 Ni^{2+} eluates were dialyzed against 20 mM Hepes and 100 mM NaCl at pH 7.0, loaded on a Mono-S column (GE Healthcare), and eluted with a linear NaCl gradient.

The identities of purified Trx1, Trx2, and Orp1 proteins were confirmed by sodium dodecyl sulfate−polyacrylamide gel electrophoresis (SDS−PAGE). Molecular masses were measured by matrix-assisted laser desorption ionization−time of flight (MALDI−TOF) mass spectrometry as described previously, where external calibration was carried out using chicken egg lysozyme C (*26*). Orp1 peroxidase activity was monitored as previously described (*12*). Oxidized Orp1 was generated by the treatment of reduced Orp1 with stoichiometric amounts of H_2O_2 under anaerobic conditions. The disulfide bonds formed in the Orp1−H_2O_2 reactions were trapped by precipitation of the oxidized protein with 20% trichloroacetic acid (TCA). The Orp1 redox state was verified with nonreducing SDS−PAGE. Initial Yap1-RD fluorescence measurements were performed using a Fluoromax-3 (Johin Yeon Horida). Yap1-RD samples were excited at 280 nm, and the fluorescence emission spectra were collected from 280 to 400 nm.

Measurement of Disulfide Bond Redox Midpoint Potentials. The redox midpoint potential (E_m) titrations for Yap1-RD, Orp1, Trx1, and Trx2 were carried out by incubation of the protein samples at defined ambient redox potential (E_h) values as described previously (*27*). Briefly, solutions with defined E_h values were prepared using mixtures of either oxidized and reduced glutathione (GSH) or oxidized and reduced dithiothreitol (DTT) (depending upon the E_h range), at a total combined concentration of 2 mM. Samples were incubated for 4 h at 25 °C prior to redox-state analysis. The titrations presented below were obtained under these conditions, but other titrations in which the total DTT or glutathione concentration was varied from 2 to 5 mM and the redox equilibration time was varied from 2 to 4 h gave essentially identical titration curves. It should also be pointed out that identical E_m values for both redox components were obtained regardless of whether the titrations were carried out aerobically or anaerobically. The redox state of Yap1-RD was quantitated by measuring changes in the intrinsic tryptophan fluorescence as a function of E_h. Fluorescence was measured using an Aminco-Bowman Series 2 luminescence spectrometer, at 1.0 nm spectral resolution, with an excitation wavelength of 275 nm and emission wavelength of 337 nm. The Orp1, Trx1, and Trx2 E_m values were quantified by labeling the protein thiols with monobromobimane (mBBr) as described previously (*28*, *29*). After the mBBr-treated protein was separated from low-molecular-mass compounds by TCA precipitation of the protein, the fluorescence of the redissolved, mBBr-labeled protein was measured and plotted as a function of E_h. Fluorescence was measured, at 1.0 nm spectral resolution, using an Aminco-Bowman Series 2 luminescent spectrometer with an excitation wavelength of 380 nm and an emission wavelength of 450 nm. The E_m values were calculated by fitting the data to the Nernst equation for a two-electron redox process. All E_m values reported represent the average from three replicate titrations. For Yap1-RD and Orp1, nonreducing SDS−PAGE was used to confirm the E_m values. For nonreducing SDS−PAGE analysis, Yap1-RD samples were incubated in 100 μL of solution poised at defined E_h values for 4 h at 25 °C. The samples were mixed with nonreducing SDS−PAGE loading buffer at ambient temperature prior to the separation on a 10−20% gradient acrylamide gel. All gels were stained with colloidal Coomassie blue (Pierce).

RESULTS

Measurement of Yap1-RD Redox Midpoint Potentials. Previous observations suggest that full-length Yap1 undergoes structural changes in response to oxidation and reduction (*20*). The intrinsic tryptophan fluorescence emission intensity increases ∼20% upon reduction of Yap1 disulfide bonds. There are three tryptophan residues in Yap1, of which only Trp602 is conserved (Figure 1A). Trp602 is also the only tryptophan located within Yap1-RD. Nuclear magnetic resonance (NMR) structure and dynamic studies indicate that in oxidized Yap1-RD Trp602 is partially buried in the Yap1-RD hydrophobic core, interacts directly with Tyr611, and is well-ordered. Upon reduction of Yap1-RD, the helix on which Trp602 is located becomes unstructured and Trp602 likely becomes exposed to the solvent. Therefore, we hypothesized that intrinsic tryptophan fluorescence could be used to measure the redox midpoint potentials of the Yap1-RD disulfide bonds.

We tested whether the intrinsic tryptophan fluorescence of Yap1-RD changes as a function of E_h and if these changes could be used to quantitatively measure the E_m value of each disulfide bond in Yap1-RD. Oxidized Yap1-RD was incubated in solutions with defined E_h values of −100, −230, or −360 mV, and the fluorescence emission spectra were measured. The fluorescence emission spectra red-shifted from a λ_{max} of 339 nm at −100 mV to a λ_{max} of 353 nm at −360 mV (Figure 1B). The λ_{max} fluorescence emission intensity increased 1.4- and 8-fold upon the change of the ambient redox potential from −100 to −230 mV and −100 to −360 mV, respectively (Figure 1B). Large changes in the intrinsic tryptophan fluorescence are consistent with the structural changes previously observed in Yap1-RD as measured by ^1H-^{15}N heteronuclear single-quantum coherence (HSQC) NMR, circular dichroism, and size-exclusion chromatography (*21*). In addition, the increases in the intrinsic tryptophan fluorescence were consistent with the changes that occurred in full-length Yap1 upon reduction (*20*). We concluded that intrinsic tryptophan fluorescence could be used to quantify the E_m values of the Yap1-RD disulfide bonds.

The E_m values for the two disulfide bonds present in Yap1-RD were measured (at pH 7.0) using GSH/oxidized glu-

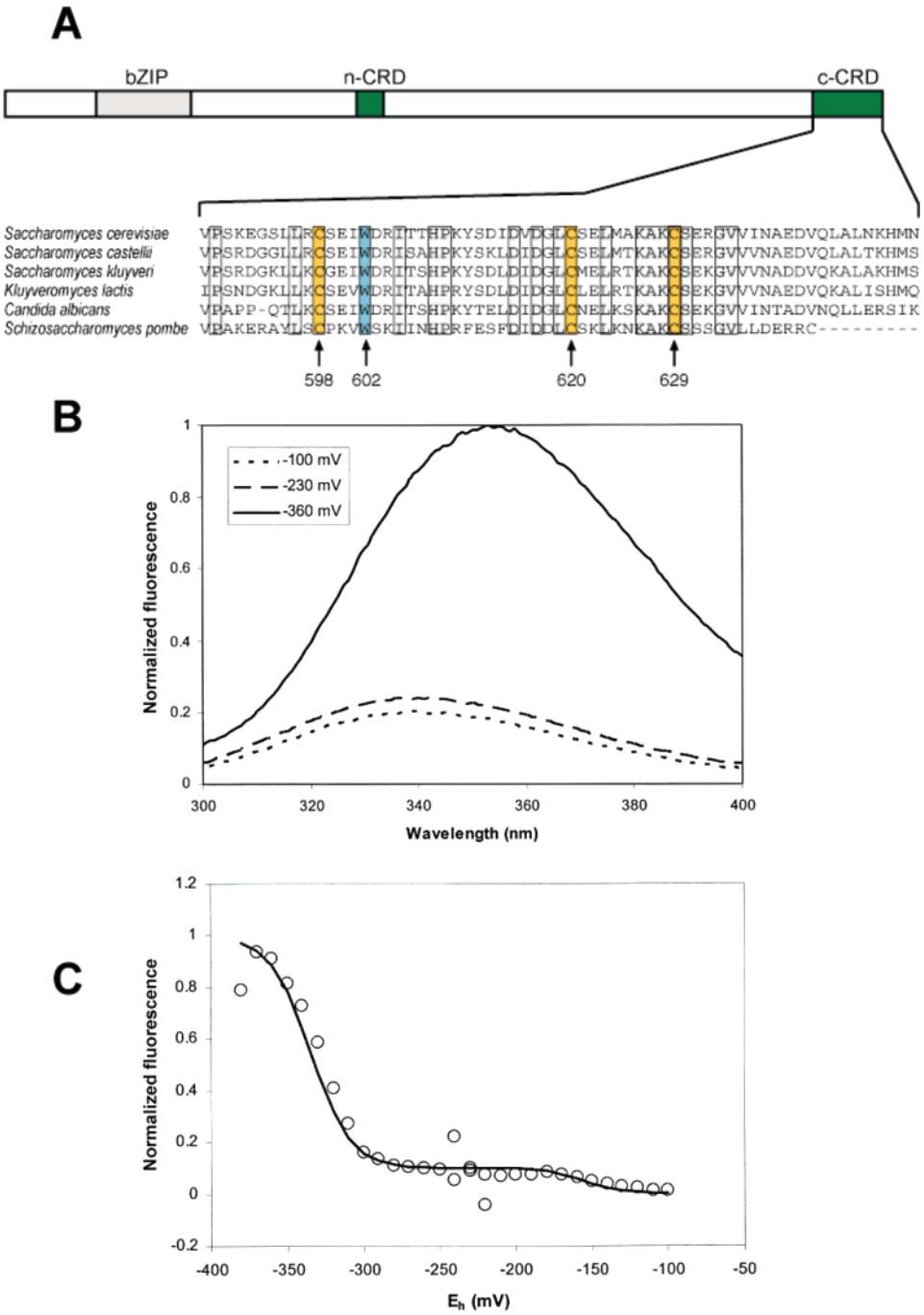

FIGURE 1: Determination of the redox midpoint potential of the Yap1-RD disulfide bonds. (A) Alignment of the c-CRD regions of six Yap1 homologues. Within the c-CRD, there are three conserved cysteine residues (yellow) and one conserved tryptophan residue (blue). (B) Samples of Yap1-RD in 100 mM Hepes at pH 7.0 were incubated in solutions with ambient redox potentials of −100, −230, and −360 mV for 4 h. A constant total glutathione or DTT concentration of 2 mM was used. After incubation at 25 °C, the intrinsic tryptophan fluorescence emission spectra were measured. (C) Yap1-RD was incubated at ambient redox potentials between −100 and −380 mV; and the intrinsic tryptophan fluorescence emission was measured at 337 nm; and the change in intensity was plotted as a function of E_h. The solid line represents best-fit, $n = 2$ Nernst curves for the −100 and −180 mV and −290 and −370 mV components of the Yap1-RD titration. The resulting E_m values from the Nernst equation fits were −155 and −330, respectively.

tathione (GSSG) redox buffers to poise samples at defined E_h values ranging from −100 to −240 mV and reduced dithiothreitol (DTT_{red})/oxidized dithiothreitol (DTT_{ox}) redox buffers to poise samples at E_h values ranging from −220 to −380 mV. Fluorescence emission spectra of the intrinsic tryptophan fluorescence were normalized and plotted as a function of E_h. Figure 1C shows that the magnitude of the tryptophan fluorescence increases in two stages, one between −100 and −180 mV and the second between −290 and −370 mV. These two portions of the titration were each fitted to the Nernst equation for a two-electron redox component. The resulting E_m values from the fit were −155 ± 3 and −330 ± 2 mV (Table 1). These results are consistent with a protein that contains two disulfide bonds, and we believe that the measured E_m values can be assigned to the Cys303−Cys598 and Cys310−Cys629 disulfide bonds in Yap1-RD.

Data from redox titrations performed at pH 6.0 also show two separate redox components that each fit well to the $n =$

Table 1: Oxidation−Reduction Midpoint Potentials

	pH 7.0		pH 6.0	
proteins	E_{m1} (mV)	E_{m2} (mV)	E_{m1} (mV)	E_{m2} (mV)
Orp1	ND[a]		−255 ± 8	
Yap-RD	−155 ± 3	−330 ± 2	−100 ± 3	−270 ± 2
Trx1	−275 ± 10		−205 ± 10	
Trx2	−265 ± 10		−215 ± 10	

[a] If we calculate the midpoint potential value at pH 7.0 based on the value observed for ORP1 at pH 6.0, then the value would be −315 ± 8 mV.

2 Nernst equation (data not shown). The E_m values at pH 6.0 were −100 ± 3 and −270 ± 2 mV (Table 1). The differences in the measured E_m values between pH 7.0 and 6.0 for both of the disulfide/dithiol couples present in Yap1-RD are equal, within the experimental uncertainties present in the measurements, to the value of −59 mV per pH unit, expected value for an uptake of 2.0 protons per disulfide bond reduced (*30*).

We used a nonreducing SDS−PAGE separation technique to provide support for our measured E_m values and to corroborate our conclusion that each E_m redox component corresponded to a Yap1-RD disulfide/dithiol couple. Yap1-RD is composed of the n-CRD and c-CRD peptides. These peptides can be resolved from Yap1-RD using SDS−PAGE under reducing conditions because of their lower molecular weight (Figure 2A). The c-CRD peptide migrates faster than Yap1-RD, with an apparent molecular mass of 10 kDa (Figure 2B). Titration over a range of E_h potentials and separation with nonreducing SDS−PAGE showed that the second disulfide bond in Yap1-RD becomes fully reduced between −320 and −340 mV (Figure 2B). While it is not possible to measure the E_m values of both disulfide bonds in Yap1-RD using this technique, the E_m value of the more reducing disulfide bond can be estimated in this fashion. The E_m value for the more reducing dithiol/disulfide couple obtained with SDS−PAGE analysis agrees, within the experimental uncertainties of the combined measurement, with the E_m value obtained using intrinsic tryptophan fluorescence.

Measurement of S. cerevisiae Thioredoxin Redox Midpoint Potentials. Previous work suggests that the cytoplasmic thioredoxins, Trx1 and Trx2, reduce the oxidized forms of Yap1 and Orp1 *in vivo* (*13*). To determine whether these reductions would be thermodynamically favorable, it was necessary to measure the E_m values for Trx1 and Trx2 and compare them with E_m values measured for Yap1-RD and Orp1. The *TRX1* and *TRX2* genes were cloned from *S. cerevisiae* and were expressed in *E. coli* with N-terminal His_6 tags. Each protein was purified to homogeneity using Ni^{2+}-affinity resin, and the molecular masses were confirmed with MALDI−TOF mass spectrometry. The redox potentials of Trx1 and Trx2 were measured at both pH 6.0 and 7.0. The results of Trx1 and Trx2 redox titrations at pH 7.0 gave good fits to the Nernst equation for a single two-electron component (parts A and B of Figure 3). The average values for Trx1 and Trx2 at pH 7.0 were −275 ± 10 and −265 ± 10 mV, respectively (Table 1). These data agree very well with previously reported E_m values ranging from −275 to −260 mV for thioredoxins (*31*−*33*). The average values for Trx1 and Trx2 at pH 6.0 were −205 ± 10 and −215 ± 10 mV, respectively (Table 1). As discussed above for the two redox components present in Yap1-RD, the differences in the measured E_m values between pH 7.0 and 6.0 for both of the thioredoxins are equal, within the experimental uncertainties present in the measurements, to the value of −59 mV per pH unit, expected value for an uptake of 2.0 protons per disulfide bond reduced (*30*).

Measurement of the Orp1 Redox Midpoint Potential. The Orp1 protein was recently identified to function as a H_2O_2 sensor that catalyzes disulfide bond formation in Yap1 (*12*).

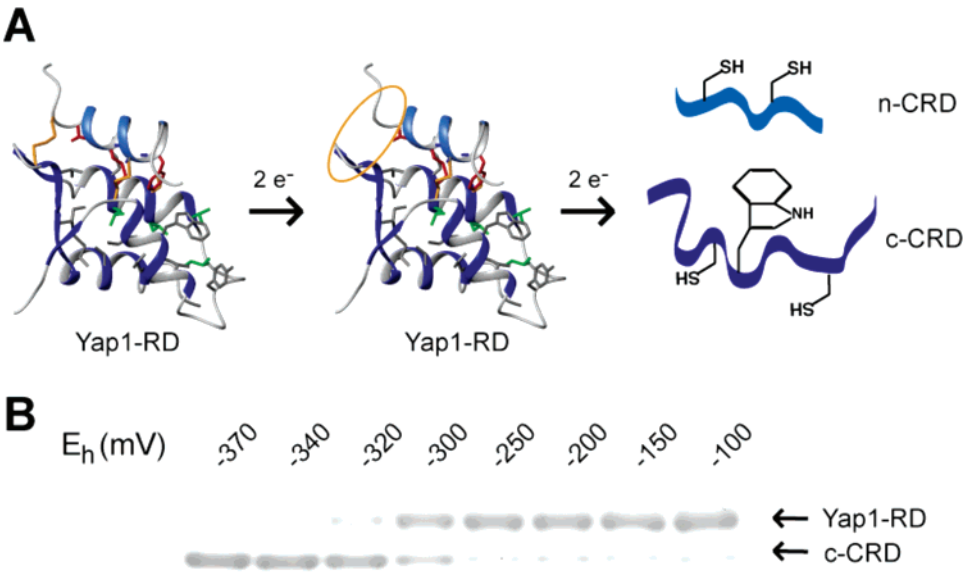

FIGURE 2: SDS−PAGE confirmation of the Yap1-RD redox midpoint potentials. (A) Structural model of the changes that occur upon reduction of each Yap1-RD disulfide bond. Reduction of the −155 mV disulfide bond results in a slight change in the overall Yap1-RD structure, which is indicated with the yellow oval. Reduction of both disulfide bonds results in the separation of the Yap1 n-CRD and c-CRD peptides and exposure of Trp602. (B) Samples of Yap1-RD were incubated in 100 mM Hepes at pH 7.0 containing 2 mM mixtures of oxidized and reduced glutathione or DTT at defined redox potentials. After 4 h at 25 °C, samples were mixed with either nonreducing or reducing SDS−PAGE loading buffer, separated on 10−20% acrylamide gels, and stained with Coomassie blue. Intact Yap1-RD and Yap1 c-CRD are observed and can be separated, but the Yap1 n-CRD did not stain with Coomassie blue. (C) Yap1-RD samples incubated over a −100 to −370 mV range of ambient redox potentials and separated by nonreducing SDS−PAGE.

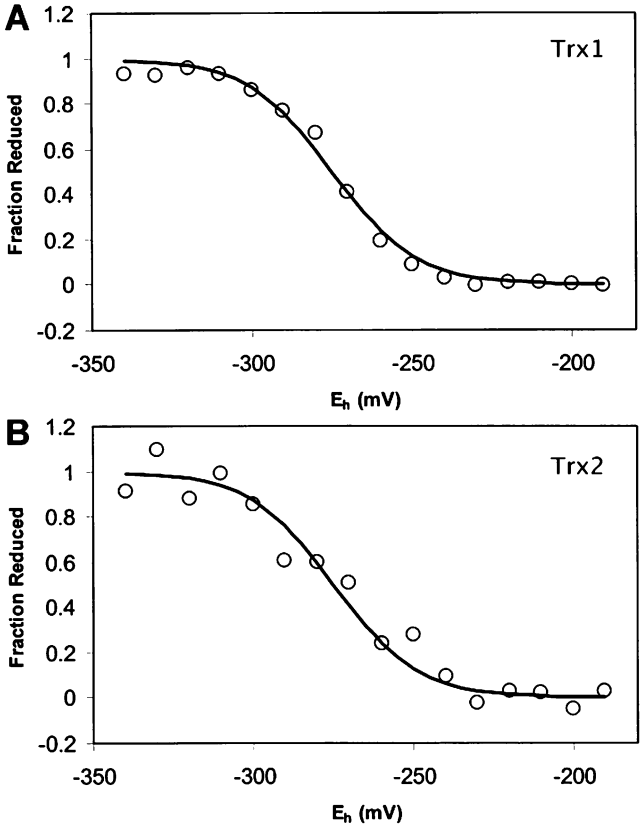

FIGURE 3: Determination of the redox midpoint potential of the *S. cerevisiae* thioredoxins. Samples of purified Trx1 (A) or Trx2 (B) were incubated in 100 mM Hepes at pH 7.0 containing mixtures of oxidized and reduced DTT at defined redox potentials. Redox equilibrium was carried out for 4 h prior to the addition of mBBr. The solid lines represent the best-fit, $n = 2$ Nernst curves, with E_m values of −275 (Trx1) and −265 mV (Trx2).

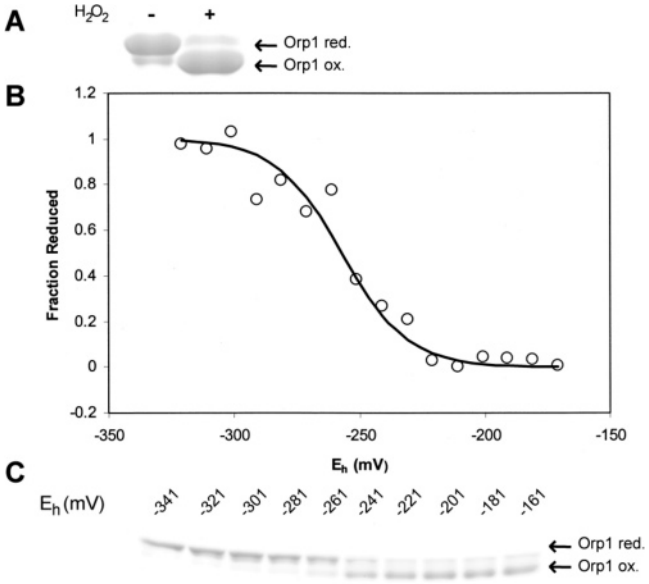

FIGURE 4: Determination of the redox midpoint potential of the Orp1 Cys36−Cys82 disulfide bond. (A) Oxidation of reduced Orp1 was carried out anaerobically by the addition of a 2-fold molar excess of H_2O_2. The reactions were stopped by the addition of TCA, and precipitated Orp1 was separated with nonreducing SDS−PAGE. Orp1 containing the Cys36−Cys82 disulfide bond migrates faster than reduced Orp1. (B) Samples of purified Orp1 were incubated in 100 mM MES at pH 6.0 containing mixtures of oxidized and reduced DTT at defined redox potentials ranging from −170 to −325 mV. Redox equilibrium was carried out for 4 h prior to the addition of mBBr. The solid line represent the best-fit, $n = 2$ Nernst curves, with an E_m values of −255 mV. (C) Orp1 incubated over a −161 to −341 mV range of ambient redox potentials and separated by nonreducing SDS−PAGE.

In addition, Orp1 has a thiol peroxidase enzymatic activity. This thiol peroxidase reaction mechanism involves an intramolecular disulfide bond intermediate between Cys36−Cys82, which is reduced by Trx1 or Trx2 *in vivo*. The *ORP1* gene was cloned from *S. cerevisiae* and expressed in *E. coli* with an N-terminal His_6 tag. The Orp1 protein was purified to homogeneity using Ni^{2+}-affinity resin, and its molecular mass was confirmed with MALDI−TOF mass spectrometry. We first measured the thiol peroxidase activity of Orp1 using a NADPH-coupled assay (*12*). In the absence of H_2O_2, there was no observed decrease in the NADPH concentration. Upon addition of H_2O_2, the N-terminally His_6-tagged Orp1 showed full peroxidase activity (data not shown). We checked for the ability of Orp1 to form the Cys36−Cys82 disulfide bond upon addition of H_2O_2. These reactions were performed with reduced Orp1 in an anaerobic hood. A 2-fold molar excess of H_2O_2 was added to Orp1, and the reaction was terminated 30 s later by the addition of 20% TCA. These conditions were designed to trap any disulfide bonds that formed in Orp1, and the reactions were separated on nonreducing SDS−PAGE. H_2O_2-Treated Orp1 migrates faster on nonreducing SDS−PAGE, with a lower apparent molecular weight, because it contains the Cys36−Cys82 disulfide bond (Figure 4A) (*12*). When H_2O_2-treated Orp1 was separated with reducing SDS−PAGE, it reverted back to the more slowly migrating species. We were also able to prepare oxidized Orp1 by dialysis under aerobic conditions. Under these conditions, oxidized Orp1 migrated with the same apparent molecular mass with SDS−PAGE as Orp1 oxidized with H_2O_2 (data not shown). Therefore, air-oxidized Orp1 was used the same as for all of the subsequent redox potential measurements.

The redox midpoint potential of Orp1 was measured at pH 6.0 using two complementary techniques (for reasons not well-understood, we were not able to obtain reproducible titration data for Orp1 at pH 7.0). Figure 4B shows the results of a redox titration carried out using redox equilibration followed by labeling of protein thiols by mBBr treatment and measurement of the fluorescence of the mBBr-labeled protein. The titration fit well with the Nernst equation for a single two-electron component with $E_m = -255 \pm 8$ mV (Table 1). The E_m value of Orp1 Cys36−Cys82 at pH 6.0 was also measured by monitoring the gel mobility of Orp1 at various E_h values (Figure 4C). As previously shown in Figure 4A, the gel motilities of oxidized and reduced Orp1 are significantly different. A transition from a slowly migrating reduced species to a faster migrating oxidized species was observed between ambient redox potentials of −261 and −241 mV. This indicates that the Orp1 Cys36−Cys82 redox midpoint potential is between these two values and supports the redox midpoint potential of -255 ± 8 mV measured with mBBr titrations.

DISCUSSION

The goal of this study was to investigate the redox midpoint potential of the disulfide bonds found in the Yap1 oxidative stress signal transduction pathway. We have

measured the redox midpoint potentials of the regulatory disulfide bonds in Yap1 and in the components of the Yap1 activation (Orp1) and deactivation pathways (Trx1 and Trx2). We prepared the Yap1-RD fragment of Yap1, which is comprised of the n-CRD and c-CRD peptides linked by disulfide bonds. Redox titrations showed that two separate two-electron redox couples are present in Yap1-RD, each with a well-defined redox midpoint potential value. We interpret these two redox midpoint potentials to correspond to the Yap1-RD disulfide bonds. We purified Orp1 and measured the redox potential of the Cys36−Cys82 disulfide bond that forms during its thiol peroxidase catalytic cycle. Finally, we purified two cytoplasmic thioredoxins, Trx1 and Trx2, and measured their redox potentials. Altogether, these measurements provide the first opportunity to examine the thermodynamic framework for redox regulation of Yap1 activity and the Orp1 peroxidase catalytic cycle.

Our E_m measurements add further support to the observation that Yap1 contains two disulfide bonds. The first and more oxidizing disulfide bond has redox midpoint potentials of −100 and −155 ± 3 mV at pH 6.0 and 7.0, respectively. The second and considerably more reducing disulfide bond has redox midpoint potentials of −270 and −330 ± 2 mV at pH 6.0 and 7.0, respectively. These measurements were made using a highly sensitive intrinsic tryptophan fluorescence assay that was based on the previously established correlation between the redox state of the disulfide/dithiol couples with the structure of Yap1-RD. At ambient redox potentials between −180 and −270 mV, there is a single two-electron reduction of a disulfide bond in Yap1-RD. The slight yet reproducible 1.4-fold increase in the intrinsic fluorescence emission suggests that there is little overall change in the Yap1-RD protein structure over this range. At ambient redox potentials lower than −330 mV, the intrinsic fluorescence changes dramatically, indicating large changes in Yap1-RD conformation and structure. This interpretation is supported by circular dichroism, size-exclusion chromatography, and NMR data (*21*). The structural changes that result from disulfide bond reduction expose the Yap1 NES and allow the Crm1 nuclear export protein to interact with Yap1.

Prior mutagenesis suggests that Cys303−Cys598 is more important for the function of Yap1 in response to H_2O_2 (*19*). For this reason, we believe that it is likely the disulfide bond with the −330 mV redox midpoint potential. In addition, mutagenesis data for the n-CRD provide additional support for this conclusion (*21*). Phe302 and Met306, which flank Cys303, provide a majority of the hydrophobic contacts between n-CRD and c-CRD. In Yap1-RD, mutation of either of these residues to alanine results in a protein that is less responsive to H_2O_2 and that cannot form stable disulfide bonds. In contrast, the mutation of Val309, which is adjacent to Cys310 and makes few hydrophobic contacts to the c-CRD, has no effect on Yap1 function (*21*). Therefore, oxidation and reduction of the Cys303−Cys598 disulfide bond appears to be the main regulation point controlling Yap1-RD structure and function. It thus seems likely that the major effects associated with changes in the redox state of Yap1 will occur over the ambient redox potential range where this disulfide bond becomes reduced.

The Trx1 and Trx2 redox midpoint potentials are very similar to those of other thioredoxins from various organisms. Previously, *S. cerevisiae* Trx1 and Trx2 were purified, and the redox midpoint potential of Trx2 was measured by Reichard and colleagues (*34*). They obtained an E_m value of −240 mV at pH 7.0 for Trx2, using an assay based on the thioredoxin reductase-catalyzed reduction of this thioredoxin by NADPH. This value is 25 mV more positive than the data collected in this study. The reasons for this difference, which are small and may well be within the combined experimental uncertainties in the two sets of measurements, are unclear.

Our data suggests that under equilibrium conditions Trx1 or Trx2 reduction of the −330 mV Yap1 disulfide bond is not a thermodynamically favorable reaction. However, *in vivo*, the concentrations of oxidized and reduced Trx1 and Trx2 are not equal. Therefore, at physiological ratios of oxidized thioredoxin (Trx_{ox})/reduced thioredoxin (Trx_{red}), the reduction of the −330 mV Yap1 disulfide bond could be thermodynamically favorable. Because Trx2 is thought to be the physiological reducing agent for Yap1, this discussion will focus on it. Previous studies demonstrate that Trx2 is kept exclusively in its reduced form *in vivo* (*35*). This occurs through the continuous reduction of the Trx2 disulfide bond, which is catalyzed by thioredoxin reductase with reducing equivalents coming from NADPH. The E_m value shown for Trx2 in Table 1 corresponds to conditions where $Trx2_{ox}$ and $Trx2_{red}$ are present at equal concentrations. In experiments designed to measure $Trx2_{ox}$ and $Trx2_{red}$ *in vivo* using TCA-based disulfide trapping assays and immunoblotting, no $Trx2_{ox}$ was observed (*35*). It is only when the cytoplasmic thioredoxin reductase gene is deleted, can quantifiable amounts of $Trx2_{ox}$ be observed (*35*). The Nernst equation can be used to estimate the redox potential of Trx2 under nonstandard conditions. Ratios of $[Trx2_{ox}]/[Trx2_{red}]$ of 10^{-2}, 10^{-3}, and 10^{-4} result in redox potentials of −324, −354, and −384 mV, respectively. Therefore, under physiological conditions, where the concentration of $Trx2_{red}$ is much greater than $Trx2_{ox}$, the effective reducing potential of Trx2 is substantially more negative than the −265 mV E_m value. This lower potential makes Trx2 reduction of the −330 mV Yap1-RD disulfide bond thermodynamically possible. In wild-type *S. cerevisiae* strains, the GSH/GSSG ratio is approximately 16 (*36*). Therefore, even under physiological GSH/GSSG ratios, where the effective redox value associated with the GSH/GSSG couple is only slightly more negative than −270 mV, GSH would be incapable of reducing the −330 mV Yap1-RD disulfide bond in a thermodynamically favorable reaction (*37*).

It is not known how the disulfide bonds in Yap1 remain oxidized over the course of 15−30 min in the overall reducing environment of the cytoplasm and nucleus (*19*). It is probable that a combination of both redox midpoint potentials and the reaction rates of disulfide bond oxidation and reduction allow for transient stability of the Yap1 disulfide bonds. Because variations in the $[Trx2_{ox}]/[Trx2_{red}]$ ratios can affect the effective reducing potential of Trx2, it tempting to speculate that this could be used to regulate the lifetime of oxidized Yap1 in the cell. For example, if the $[Trx2_{ox}]/[Trx2_{red}]$ ratios were to increase in response to oxidative stress, oxidized Yap1 could survive in the cell until the $[Trx2_{ox}]/[Trx2_{red}]$ ratio was restored back to nonstressed levels. Full restoration of the nonstressed $[Trx2_{ox}]/[Trx2_{red}]$ ratio may not occur until Yap1 has activated the expression

of antioxidant genes required to protect against oxidative stress. Thus, this time frame would give Yap1 a 10−20 min window to remain oxidized and activate antioxidant gene expression.

Orp1 was originally annotated as a glutathione peroxidase based on protein-sequence homology. Delaunay et al. showed that the Orp1 Cys36−Cys82 disulfide bond is essential for its thiol peroxidase activity and that this specific disulfide bond was reduced by Trx2 *in vivo* (*12*). We have measured the Orp1 Cys36−Cys82 redox midpoint potential of −255 mV at pH 6.0 (as indicated above, unexplained problems prevented measuring an E_m value at pH 7.0). If one assumes that Orp1 does not contain any redox-linked acid/base groups with pK_a values between 6.0 and 7.0, one can extrapolate from the value measured at pH 6.0 to a likely value of −314 mV at pH 7.0 (i.e., assuming the E_m versus pH profile has the −59 mV per pH unit value expected for a process in which the uptake of two protons accompanies the reduction of a disulfide bond). An E_m value of −314 mV is too negative for reduction by the GSH/GSSG couple. Using the same reasoning as we did for Yap1 reduction, a sufficiently low $[Trx2_{ox}]/[Trx2_{red}]$ ratio would create conditions where Cys36−Cys82 reduction would be thermodynamically favorable. In the future, the redox midpoint potential of the Cys36−Cys598 mixed disulfide bond between Orp1 and Yap1 needs to be examined to provide a thermodynamic explanation for Orp1 catalysis of the Yap1 disulfide bonds.

ACKNOWLEDGMENT

M.J.W. acknowledges Gisela Storz for support during this research. We also thank Christina Takanishi for critical reading of our manuscript. Work carried out at Texas Tech University was supported by a grant (D-0710 to D.B.K.) from the Robert A. Welch Foundation.

REFERENCES

1. Kasai, H. (1997) Analysis of a form of oxidative DNA damage, 8-hydroxy-2′-deoxyguanosine, as a marker of cellular oxidative stress during carcinogenesis, *Mutat. Res. 387*, 147−163.
2. Oliver, C. N., Starke-Reed, P. E., Stadtman, E. R., Liu, G. J., Carney, J. M., and Floyd, R. A. (1990) Oxidative damage to brain proteins, loss of glutamine synthetase activity, and production of free radicals during ischemia/reperfusion-induced injury to gerbil brain, *Proc. Natl. Acad. Sci. U.S.A. 87*, 5144−5147.
3. Reznick, A. Z., and Packer, L. (1994) Oxidative damage to proteins: Spectrophotometric method for carbonyl assay, *Methods Enzymol. 233*, 357−363.
4. Vile, G. F., and Tyrrell, R. M. (1995) Uva radiation-induced oxidative damage to lipids and proteins in vitro and in human skin fibroblasts is dependent on iron and singlet oxygen, *Free Radical Biol. Med. 18*, 721−730.
5. Cerutti, P., and Trump, B. (1991) Inflammation and oxidative stress in carcinogenesis, *Cancer Cells 3*, 1−7.
6. Klaunig, J. E., Xu, Y., Isenberg, J. S., Bachowski, S., Kolaja, K. L., Jiang, J., Stevenson, D. E., and Walborg, E. F. (1998) The role of oxidative stress in chemical carcinogenesis, *Environ. Health Perspect. 106*, 289−295.
7. Trush, M. A., and Kensler, T. W. (1991) An overview of the relationship between oxidative stress and chemical carcinogenesis, *Free Radical Biol. Med.* 201−209.
8. Carmel-Harel, O., and Storz, G. (2000) Roles of the glutathione- and thioredoxin-dependent reduction systems in the *Escherichia coli* and *Saccharomyces cerevisiae* responses to oxidative stress, *Annu. Rev. Microbiol. 54*, 439−461.
9. Storz, G., and Imlay, J. A. (1999) Oxidative stress, *Curr. Opin. Microbiol. 2*, 188−194.
10. Storz, G., and Zheng, M. (2000) Oxidative stress, in *Bacterial Stress Response* (Storz, G., and Hengge-Aronis, R., Eds.) ASM Press, Washington, DC.
11. Carmel-Harel, O., Wood, M. J., and Storz, G. (2003) Regulatory disulfides controlling transcription factor activity in the bacterial and yeast responses to oxidative stress, in *In Celluar Implications of Redox Signaling* (Gitler, C., and A., D., Eds.) pp 287−310, Imperial College Press, London, U.K.
12. Delaunay, A., Pflieger, D., Barrault, M. B., Vinh, J., and Toledano, M. B. (2002) A thiol peroxidase is an H_2O_2 receptor and redox-transducer in gene activation, *Cell 111*, 471−481.
13. Izawa, S., Maeda, K., Sugiyama, K., Mano, J., Inoue, Y., and Kimura, A. (1999) Thioredoxin deficiency causes the constitutive activation of Yap1 an AP-1-like transcription factor in *Saccharomyces cerevisiae*, *J. Biol. Chem. 274*, 28459−28465.
14. Veal, E. A., Ross, S. J., Malakasi, P., Peacock, E., and Morgan, B. A. (2003) Ybp1 is required for the hydrogen peroxide-induced oxidation of the Yap1 transcription factor, *J. Biol. Chem. 278*, 30896−30904.
15. Gasch, A. P., Spellman, P. T., Kao, C. M., Carmel-Harel, O., Eisen, M. B., Storz, G., Botstein, D., and Brown, P. O. (2000) Genomic expression programs in the response of yeast cells to environmental changes, *Mol. Biol. Cell. 11*, 4241−4257.
16. Kuge, S., Jones, N., and Nomoto, A. (1997) Regulation of yAP-1 nuclear localization in response to oxidative stress, *EMBO J. 16*, 1710−1720.
17. Isoyama, T., Murayama, A., Nomoto, A., and Kuge, S. (2001) Nuclear import of the yeast AP-1-like transcription factor Yap1p is mediated by transport receptor Pse1p, and this import step is not affected by oxidative stress, *J. Biol. Chem. 276*, 21863−21869.
18. Yan, C., Lee, L. H., and Davis, L. I. (1998) Crm1p mediates regulated nuclear export of a yeast AP-1-like transcription factor, *EMBO J. 17*, 7416−7429.
19. Delaunay, A., Isnard, A. D., and Toledano, M. B. (2000) H_2O_2 sensing through oxidation of the Yap1 transcription factor, *EMBO J. 19*, 5157−5166.
20. Wood, M. J., Andrade, E. C., and Storz, G. (2003) The redox domain of the Yap1p transcription factor contains two disulfide bonds, *Biochemistry 42*, 11982−11991.
21. Wood, M. J., Storz, G., and Tjandra, N. (2004) Structural basis for redox regulation of Yap1 transcription factor localization, *Nature 430*, 917−921.
22. Wood, Z. A., Poole, L. B., and Karplus, P. A. (2003) Peroxiredoxin evolution and the regulation of hydrogen peroxide signaling, *Science 300*, 650−653.
23. Avery, A. M., and Avery, S. V. (2001) *Saccharomyces cerevisiae* expresses three phospholipid hydroperoxide glutathione peroxidases, *J. Biol. Chem. 276*, 33730−33735.
24. Carmel-Harel, O., Stearman, R., Gasch, A. P., Botstein, D., Brown, P. O., and Storz, G. (2001) Role of thioredoxin reductase in the Yap1p-dependent response to oxidative stress in *Saccharomyces cerevisiae*, *Mol. Microbiol. 39*, 595−605.
25. Godon, C., Lagniel, G., Lee, J., Buhler, J. M., Kieffer, S., Perrot, M., Boucherie, H., Toledano, M. B., and Labarre, J. (1998) The H_2O_2 stimulon in *Saccharomyces cerevisiae*, *J. Biol. Chem. 273*, 22480−22489.
26. Kim, S. K., Rahman, A., Bick, J. A., Conover, R. C., Johnson, M. K., Mason, J. T., Hirasawa, M., Leustek, T., and Knaff, D. B. (2004) Properties of the cysteine residues and iron−sulfur cluster of the assimilatory 5′-adenylyl sulfate reductase from *Pseudomonas aeruginosa*, *Biochemistry 43*, 13478−13486.
27. Setterdahl, A., Hirasawa, M., Bucher, L. M., Dholakia, C. A., Jacquot, P., Yards, H., Miller, F., Stevens, F. J., Knaff, D. B., and Anderson, L. E. (2000) Oxidation−reduction properties of two engineered redox-sensitive mutant *Escherichia coli* malate dehydrogenases, *Arch. Biochem. Biophys. 382*, 15−21.
28. Hirasawa, M., Schurmann, P., Jacquot, J. P., Manieri, W., Jacquot, P., Keryer, E., Hartman, F. C., and Knaff, D. B. (1999) Oxidation−reduction properties of chloroplast thioredoxins, ferredoxin: thioredoxin reductase, and thioredoxin f-regulated enzymes, *Biochemistry 38*, 5200−5205.
29. Krimm, I., Lemaire, S., Ruelland, E., Miginiac-Maslow, M., Jaquot, J. P., Hirasawa, M., Knaff, D. B., and Lancelin, J. M. (1998) The single mutation Trp35 → Ala in the 35−40 redox site of *Chlamydomonas reinhardtii* thioredoxin h affects its biochemical activity and the pH dependence of C36−C39 ^1H-^{13}C NMR, *Eur. J. Biochem. 255*, 185−195.
30. Setterdahl, A. T., Chivers, P. T., Hirasawa, M., Lemaire, S. D., Keryer, E., Miginiac-Maslow, M., Kim, S. K., Mason, J., Jacquot,

J. P., Longbine, C. C., de Lamotte-Guery, F., and Knaff, D. B. (2003) Effect of pH on the oxidation−reduction properties of thioredoxins, *Biochemistry 42*, 14877−14884.
31. Krause, G., Lundstrom, J., Barea, J. L., Pueyo de la Cuesta, C., and Holmgren, A. (1991) Mimicking the active site of protein disulfide-isomerase by substitution of proline 34 in *Escherichia coli* thioredoxin, *J. Biol. Chem. 266*, 9494−9500.
32. Moore, E. C., Reichard, P., and Thelander, L. (1964) Enzymatic synthesis of deoxyribonucleotides. V. Purification and properties of thioredoxin reductase from *Escherichia coli* B, *J. Biol. Chem. 239*, 3445−3452.
33. Salamon, Z., Gleason, F. K., and Tollin, G. (1992) Direct electrochemistry of thioredoxins and glutathione at a lipid bilayer-modified electrode, *Arch. Biochem. Biophys. 299*, 193−198.
34. Gonzalez Porque, P., Baldesten, A., and Reichard, P. (1970) Purification of a thioredoxin system from yeast, *J. Biol. Chem. 245*, 2363−2370.
35. Trotter, E. W., and Grant, C. M. (2005) Overlapping roles of the cytoplasmic and mitochondrial redox regulatory systems in the yeast *Saccharomyces cerevisiae*, *Eukaryotic Cell 4*, 392−400.
36. Muller, E. G. (1996) A glutathione reductase mutant of yeast accumulates high levels of oxidized glutathione and requires thioredoxin for growth, *Mol. Biol. Cell. 7*, 1805−1813.
37. Rost, J., and Rapoport, S. (1964) Reduction potential of glutathione, *Nature 201*, 185.

BI061136Y